

# Mathematical modeling of wildland fire initiation and spread

Vladimir Agranat<sup>a,\*</sup>, Valeriy Perminov<sup>b</sup>

<sup>a</sup> Applied Computational Fluid Dynamics Analysis, Thornhill, Ontario, Canada

<sup>b</sup> Tomsk Polytechnic University, Tomsk, Russia

## ARTICLE INFO

### Keywords:

Wildland fire  
Combustion  
Rate of spread  
Software

## ABSTRACT

The aim of this paper is to create a user-friendly computational tool for analysis of wildland fire behavior and its effect on urban and other structures. A physics-based multiphase Computational Fluid Dynamics (CFD) model of wildfire initiation and spread has been developed and incorporated into the multi-purpose CFD software, PHOENICS. It accounts for all the important physicochemical processes: drying, pyrolysis, char combustion, turbulent combustion of gaseous products of pyrolysis, exchange of mass, momentum and energy between gas and solid phase, turbulent flow and convective, conductive and radiative heat transfer. Turbulence is modeled by using a RNG  $k-\epsilon$  model and the radiative heat transfer is represented by the IMMERSOL model. The Arrhenius-type kinetics are used for heterogeneous reactions and the eddy-breakup approach is applied for gaseous combustion. The model has been validated using the experimental data.

## 1. Introduction

Wildland fires are extremely complex and destructive phenomena and their behavior depends on the state of vegetation, meteorological conditions and ground terrain. Experimental studies of wildfire behavior are expensive and challenging tasks. This makes the development of robust and accurate models of wildfire behavior an extremely important activity. There are various types of wildland fire models: statistical, empirical, semi-empirical and physics-based. This paper is devoted to the development and validation of a physics-based multiphase Computational Fluid Dynamics (CFD) model of wildland fire initiation and spread and smoke dispersion.

Over the past 30 years, significant progress in the development of physics-based wildfire models has been achieved. In particular, fully physical multiphase wildfire models have been developed by Grishin et al. (1986), Grishin (1997), Porterie et al. (1998, 2000, 2005), Morvan and Dupuy (2001), and Mell et al. (2007).

According to a review by Morvan (2011), one of the most advanced fully physical multiphase wildfire models is the three-dimensional (3D) model, WFDS (Wildland urban interface Fire Dynamics Simulator), developed at the Building and Fire Research Laboratory (BFRL) of NIST. The validation of WFDS is ongoing: its recent validation was conducted by Menage et al. (2012) by using the experimental data of Mendes-Lopes et al. (2003) on surface fire propagation in a bed of *Pinus pinaster* needles. The same set of data was also used by Porterie et al. (2000) in

validating their multiphase model.

In recent years, a number of experimental and theoretical works have been performed by El Houssami et al. (2016, 2018), Padhi et al. (2016), and Frangieha et al. (2018)) to study the combustion of different porous wildland fuels. Numerical simulations were compared to laboratory experiments carried out with porous pine needles beds (El Houssami et al. (2016, 2018)), shrub fuels (Padhi et al. (2016)) and grass (Frangieha et al. (2018)). The relevance of various sub-models used to close the multiphase CFD models was assessed.

The process of forest fire propagation was analyzed by Grishin (1997) and Perminov (2013) with use of simplified two-dimensional (2D) multiphase formulation. The equations of three-dimensional (3D) model were integrated by these researchers over the height of the forest canopy and the resulting 2D system of equations was solved to study the dynamics of wildfire spread and the preventive measures such as fire breaks and barriers. The dynamic turbulent viscosity was determined using simplified local equilibrium model of turbulence (Grishin, 1997) and the Arrhenius-type kinetics were applied for both heterogeneous reactions and gaseous combustion.

In the present study, a fully physical multiphase 3D model of wildland fire behavior was developed and incorporated into the commercial general-purpose CFD software, PHOENICS, employed as a framework and a solver (<http://www.cham.co.uk/phoenics.php>). The model contains the main features proposed by previous researchers, i.e. Grishin (1997) and Porterie et al. (1998, 2000), and it accounts for all the

\* Corresponding author.

E-mail addresses: [vlad@acfd.org](mailto:vlad@acfd.org) (V. Agranat), [perminov@tpu.ru](mailto:perminov@tpu.ru) (V. Perminov).

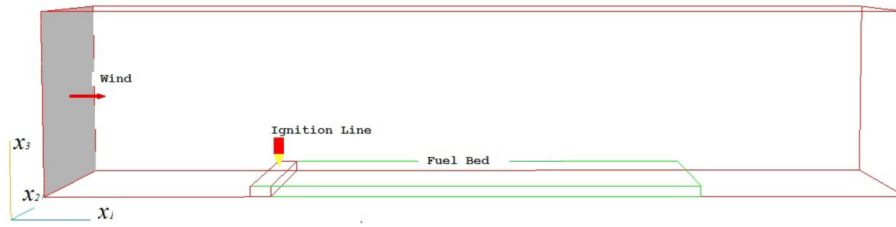


Fig. 1. Computational domain: wind, ignition line and fuel bed.

Table 1

Dependent variables, effective exchange coefficients and source terms in equation (1).

Conservation of	$\phi$	$\Gamma_\phi$	$S_\phi$
Mass	1	0	$\dot{m}$
$x_i$ – momentum	$u_i$	$\mu + \mu_t$	$-\frac{\partial p^i}{\partial x_i} + (\rho - \rho_e)g_i - \frac{1}{8}A_s C_d \rho u_i  \vec{u} $
Enthalpy	$h$	$\frac{\mu}{Pr} + \frac{\mu_t}{Pr_t}$	$m_5 q_5 - A_s h_s (T - T_s) + 4\epsilon_1 \sigma (T_3^4 - T^4)$
Mass of $\alpha$ – species	$c_\alpha$	$\frac{\mu}{Sc} + \frac{\mu_t}{Sc_t}$	$m_{5\alpha}$
Turbulent kinetic energy	$k$	$\mu + \frac{\mu_t}{\sigma_k}$	$\rho(P_k + W_k - \epsilon)$
Dissipation rate of turbulent kinetic energy	$\epsilon$	$\mu + \frac{\mu_t}{\sigma_\epsilon}$	$\rho \frac{\epsilon}{k} (C_{\epsilon 1} P_k - C_{\epsilon 2} \epsilon + C_{\epsilon 3} W_k - R_{RNG})$

important physical and physicochemical processes: drying, pyrolysis, char combustion, turbulent combustion of gaseous products of pyrolysis, exchange of mass, momentum and energy between gas and solid phase, turbulent gas flow and convective, conductive and radiative heat transfer. The use of PHOENICS software as a framework for modeling allows model applications by potential users (students, researchers, fire management teams, etc.) without any special CFD background due to availability of user-friendly software interface, documentation and technical support. Moreover, an open and general structure of software enables users to modify the model, test various built-in models of turbulence and radiation, try various numerical schemes and import geometries from CAD packages in order to model complex shapes of objects in wildland-urban interface (WUI).

The novelty of the current paper relative to the previous studies is that a physics-based multiphase 3D wildfire model, which is based on available data on chemical kinetics of heterogeneous reactions, eddy-break-up approach for gaseous combustion, RNG  $k-\epsilon$  turbulence model and IMMERSOL radiation model, has been incorporated for the first time into the general-purpose CFD software and validated using the

experimental data of Mendes-Lopes et al. (2003) on surface fire propagation in a bed of pine needles. In the following sections, the physical and mathematical formulation is presented (section 2), the numerical method is described (section 3) and the simulation results are discussed and compared with experimental data (section 4).

## 2. Physical and mathematical formulation

### 2.1. Modeling assumptions

Following a multiphase modeling approach proposed by Grishin (1997) and Porterie et al. (2000) the forest is considered in this paper as a chemically reactive multiphase medium containing gas phase with a volume fraction of  $\varphi_g$  and condensed phase with a volume fraction of  $\varphi_s$  (liquid water, dry organic matter, solid pyrolysis products and mineral part of fuel). The interaction between phases is modeled by two sets of phase governing equations linked with proper source terms expressing the gas flow resistance, multiphase heat transfer and chemical reactions. The model accounts for drying, pyrolysis, char combustion, turbulent combustion of gaseous products of pyrolysis, turbulent gas flow and heat transfer. In this study, the radiative heat transfer is modeled by means of the IMMERSOL model (Spalding, 1995, 2013), which is essentially an extension of the P-1 approximation to handle optically-thin, as well as optically-thick media, and soot formation is ignored. The Arrhenius-type kinetics are used for heterogeneous reactions (drying, pyrolysis and char combustion) and the eddy dissipation concept (EDC) of Magnussen and Hjertager (1976) is applied for modeling the gaseous combustion. Turbulence is modeled by using the renormalization group (RNG)  $k-\epsilon$  model (Yakhot and Smith (1992)).

As proposed by Grishin et al. (1986), Grishin (1997) and Porterie et al. (1998, 2000, 2005) the degradation of the solid fuel via drying, pyrolysis and char combustion and the combustion of volatiles arising from the pyrolysis process is summarized in the present study by the following simplified four-step reaction mechanism:

#### 1. Endothermic drying reaction

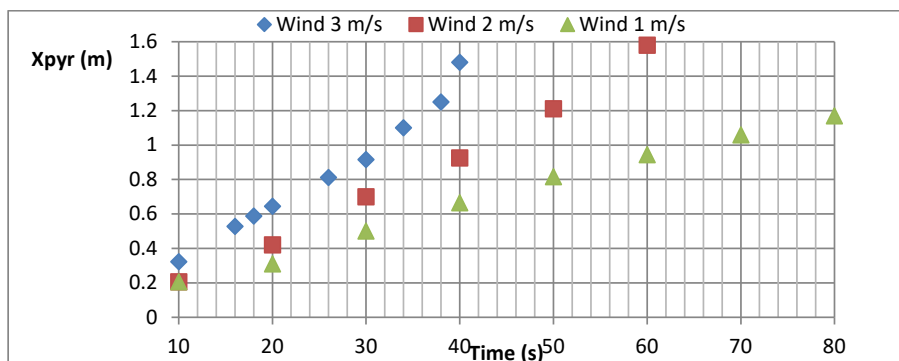
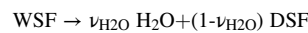


Fig. 2. Pyrolysis front propagation for three wind speeds of 1, 2 and 3 m/s.

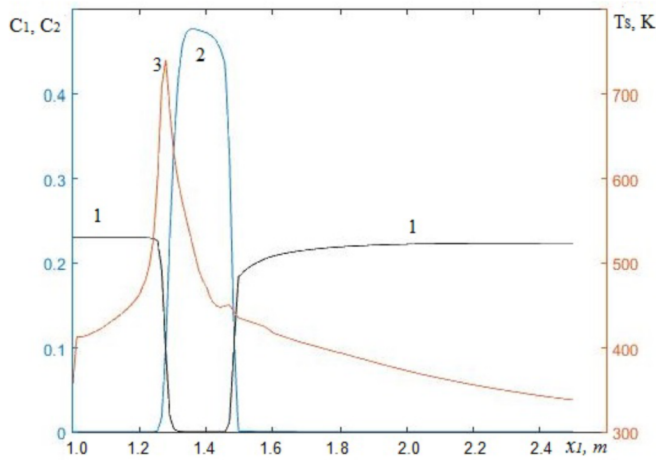


Fig. 3. Solid phase temperature (3) and mass fractions of oxygen (1) and carbon monoxide (2) for wind speed of 1 m/s at  $t = 20$  s.

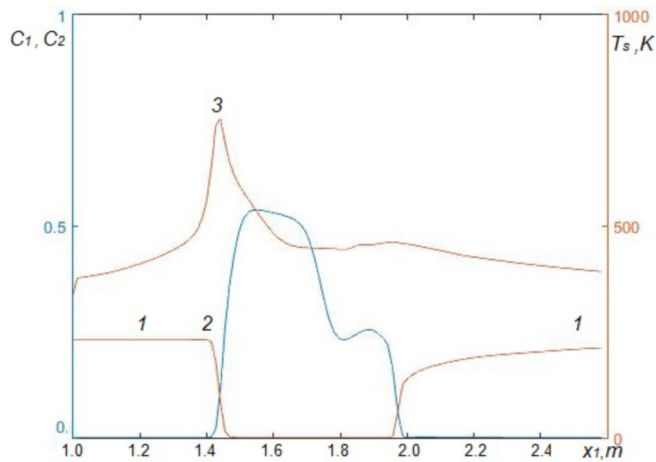
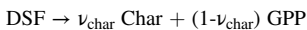


Fig. 4. Solid phase temperature (3) and mass fractions of oxygen (1) and carbon monoxide (2) for wind speed of 2 m/s at  $t = 20$  s.

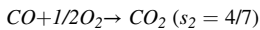
## 2. Endothermic pyrolysis reaction



## 3. Exothermic charcoal oxidation (carbon combustion)



## 4. Exothermal oxidation of combustible gaseous pyrolysis products (CO combustion)



where *WSF*, *DSF* and *GPP* symbolize the wet solid fuel, dry solid fuel and gaseous pyrolysis products respectively (written in mass);  $\nu_{H_2O}$  and  $\nu_{char}$  are the stoichiometric coefficients for drying and pyrolysis;  $s_1$  and  $s_2$  are the stoichiometric ratios for heterogeneous and homogeneous reactions.

As a consequence of pyrolysis, char and gaseous pyrolysis products (*GPP*) are formed. Soot is neglected as its mass fraction is less than 1% of the total mass of soot and gaseous mixture (Porter et al. (2005)). Char consists of pure carbon (80–97%) and ash. *GPP* include combustible and noncombustible parts. It is assumed in the above mechanism that char is pure carbon (C) and the combustible part of *GPP* is an effective gas of the CO type. The CO combustion reaction is assumed to be infinite fast and the local CO burning rate is taken to be the lowest of the turbulence

dispersion rates of either fuel (CO) or oxygen (Magnussen and Hjertager (1976) and Morvan and Dupuy (2001)). The gas phase is simplified as a mixture of five major components:  $O_2$ , CO,  $CO_2$ ,  $H_2O$  and  $N_2$ .

Fig. 1 shows the 3D domain containing the gas flow region, a fuel bed representing the forest and an ignition line. The specific sizes of domain and fuel bed vary in various case studies.

## 2.2. Gas-phase equations

The gas phase governing equations are written in a generic form as follows:

$$\frac{\partial}{\partial t}(\rho\Phi) + \frac{\partial}{\partial x_i} \left( \rho u_i \Phi - \Gamma_\phi \frac{\partial \Phi}{\partial x_i} \right) = S_\phi \quad (1)$$

Here,  $t$  is the time;  $x_i$  is the spacial coordinate ( $i = 1, 2, 3$ );  $\rho$  is the gas mixture density;  $u_i$  is the velocity component in  $x_i$  direction and the specific expressions for dependent variable,  $\Phi$ , diffusive exchange coefficient,  $\Gamma_\phi$ , and source term,  $S_\phi$ , are given in Table 1 below. The gas phase volume fraction,  $\varphi_g$ , is taken equal to unity in equation (1) as  $\varphi_g = 1 - \varphi_s$ , where the volume fraction of condensed phase,  $\varphi_s$ , is very small in the present study ( $\varphi_s < 0.016$ ). The gas density is calculated from the ideal gas law equation of state for mixture of gases:

$$p = \rho RT \sum_{\alpha=1}^3 \frac{c_\alpha}{M_\alpha}$$

where  $p$  is the gas pressure;  $T$  is the absolute gas temperature;  $R$  is the universal gas constant;  $c_\alpha$  is the mass fraction of  $\alpha$ -species of gas mixture; index  $\alpha = 1, 2, 3$ , where 1 corresponds to oxygen, 2 - to carbon monoxide, 3 - to all other components of the gas mixture ( $\sum_{\alpha=1}^3 c_\alpha = 1$ );  $M_\alpha$

is the molecular weight of  $\alpha$ -component of gas phase.

Here,  $h$  is the gas enthalpy;  $k$  is the turbulent kinetic energy;  $\varepsilon$  is the dissipation rate of turbulent kinetic energy;  $\mu$  and  $\mu_t$  are the dynamic molecular and turbulent viscosities calculated from equations:  $\mu = \frac{1.479 \cdot 10^{-6} T^{1.5}}{(T+116.275)}$ ,  $\mu_t = C_\mu \rho k^2 / \varepsilon$ ;  $Pr$ ,  $Sc$ ,  $Pr_t$  and  $Sc_t$  are the molecular and turbulent Prandtl and Schmidt numbers ( $Pr = 1005\mu / 0.0258$ ,  $Sc = Pr_t = Sc_t = 1$ );  $\bar{\sigma}_k$ ,  $\bar{\sigma}_\varepsilon$ ,  $C_{\mu\nu}$ ,  $C_{\varepsilon 1}$ ,  $C_{\varepsilon 2}$ ,  $C_{\varepsilon 3}$  are the empirical constants of turbulent model ( $\bar{\sigma}_k = 0.7194$ ,  $\bar{\sigma}_\varepsilon = 0.7194$ ,  $C_{\mu\nu} = 0.0845$ ,  $C_{\varepsilon 1} = 1.42$ ,  $C_{\varepsilon 2} = 1.68$ ,  $C_{\varepsilon 3} = 1.0$ );  $g_i$  is the gravity acceleration component ( $\vec{g} = (0, 0, -g)$ ) in the term of momentum equation that describes the buoyancy forces;  $\rho_e$  is the reference density and  $p'$  is the pressure perturbation relative to the hydrostatic reference condition;  $\vec{u}$  is the gas velocity vector having three velocity components  $u_1, u_2, u_3$ ;  $A_s$  is the specific wetted area of fuel bed ( $A_s = \varphi_s \sigma_s$ );  $\sigma_s$  is the surface-area-to-volume ratio of solid particle;  $C_d$  is a particle drag coefficient ( $C_d = 24(1 + 0.15 Re_{es}^{0.687}) / Re_{es}$ ,  $Re_{es} < 800$ ) depending on the effective particle Reynolds number,  $Re_{es} = \rho |\vec{u}| d_{es} / \mu$ , which is calculated using the equivalent spherical particle diameter,  $d_{es} = 6 / \sigma_s$ ;  $h_s$  is the particle heat transfer coefficient ( $h_s = \lambda Nu_s / d_s$ ) depending on the heat conductivity of gas,  $\lambda$ , particle Nusselt number,  $Nu_s$ , and equivalent diameter of cylindrical particle,  $d_s = 4 / \sigma_s$ ;  $Nu_s$  is a function of particle Reynolds number,  $Re_s = \rho |\vec{u}| d_s / \mu$ :  $Nu_s = 0.683 Re_s^{0.466}$ ;  $q_5$  is the heat effect of gas phase combustion of carbon monoxide ( $q_5 = 10^7$  J/kg);  $\sigma$  is the Stefan-Boltzman constant;  $T_3$  is the absolute temperature of solid phase;  $T_3$  is the 'radiosity temperature' defined as  $(R_l / (4\sigma))^{1/4}$ , where  $R_l$  is the incident radiation ( $Wm^{-2}$ );  $\varepsilon_j$  is the absorption coefficient of gas phase;  $R_{RNG}$  is an additional term proposed in the RNG  $k$ - $\varepsilon$  model by Yakhot and Smith (1992);  $P_k$  and  $W_k$  are the turbulence production/destruction terms defined by Launder and Spalding (1974);  $P_k$  is the volumetric production rate of  $k$  by shear forces and  $W_k$  is the volumetric production rate of  $k$  by gravitational forces interacting with density gradients.

It should be mentioned that the energy equation was formulated in terms of temperature rather than enthalpy using a link between enthalpy and temperature:  $dh = C_p dT$ , where  $C_p$  is the specific heat of gas mixture. The specific heat was involved in convection and transient terms and thermal conductivity,  $k_g$ , entered as a multiplier of

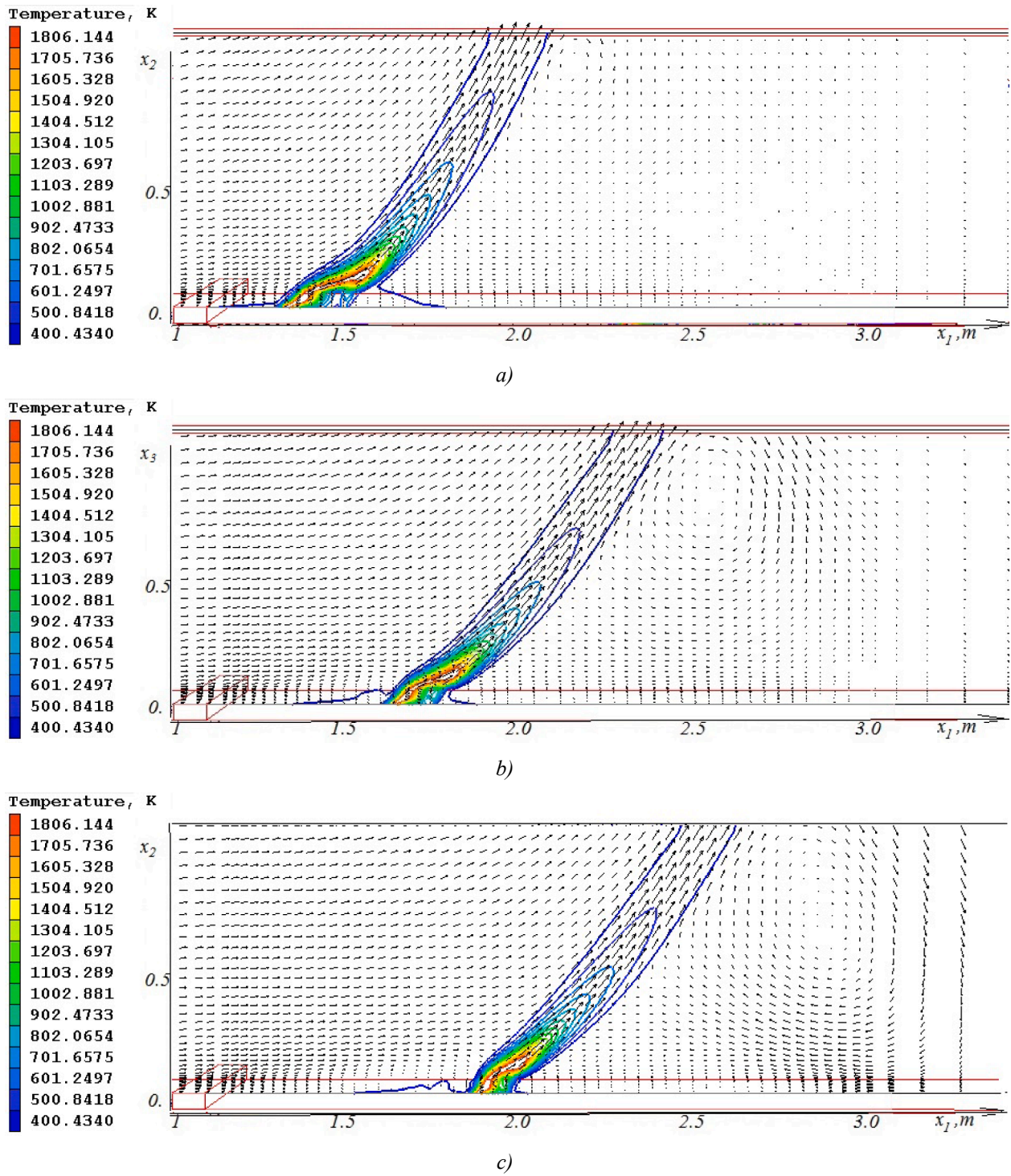


Fig. 5. Gas temperature and velocity vectors at wind speed of 1 m/s.

temperature gradient in heat conduction terms. A constant value of  $k_g$  equal to  $0.0258 \text{ Wm}^{-1}\text{K}^{-1}$  and a constant value of  $Cp_g$ , equal to  $1005 \text{ Jkg}^{-1}\text{K}^{-1}$  were used in the present work for simplicity. The future studies will account for dependencies of  $k_g$  and  $Cp_g$  on gas composition and temperature.

The mass production/consumption rates  $\dot{m}$ ,  $m_5$ ,  $m_{51}$  and  $m_{52}$  are defined as the following (Grishin (1997) and Porterie et al. (2000)):

$$\dot{m} = (1 - \alpha_c)R_1 + R_2 + \frac{M_C}{M_1}R_3 \quad (2)$$

$$m_5 = \frac{4\rho\varepsilon}{k} \min\left(c_2, \frac{c_1}{s_2}\right) \quad (3)$$

$$m_{51} = -\frac{1}{2} \frac{M_1}{M_2} m_5 - R_3 \quad (4)$$

$$m_{52} = \nu_g(1 - \alpha_c)R_1 - m_5 \quad (5)$$

$$R_1 = k_1 \rho_1 \phi_1 \exp(-E_1 / RT_S) \quad (6)$$

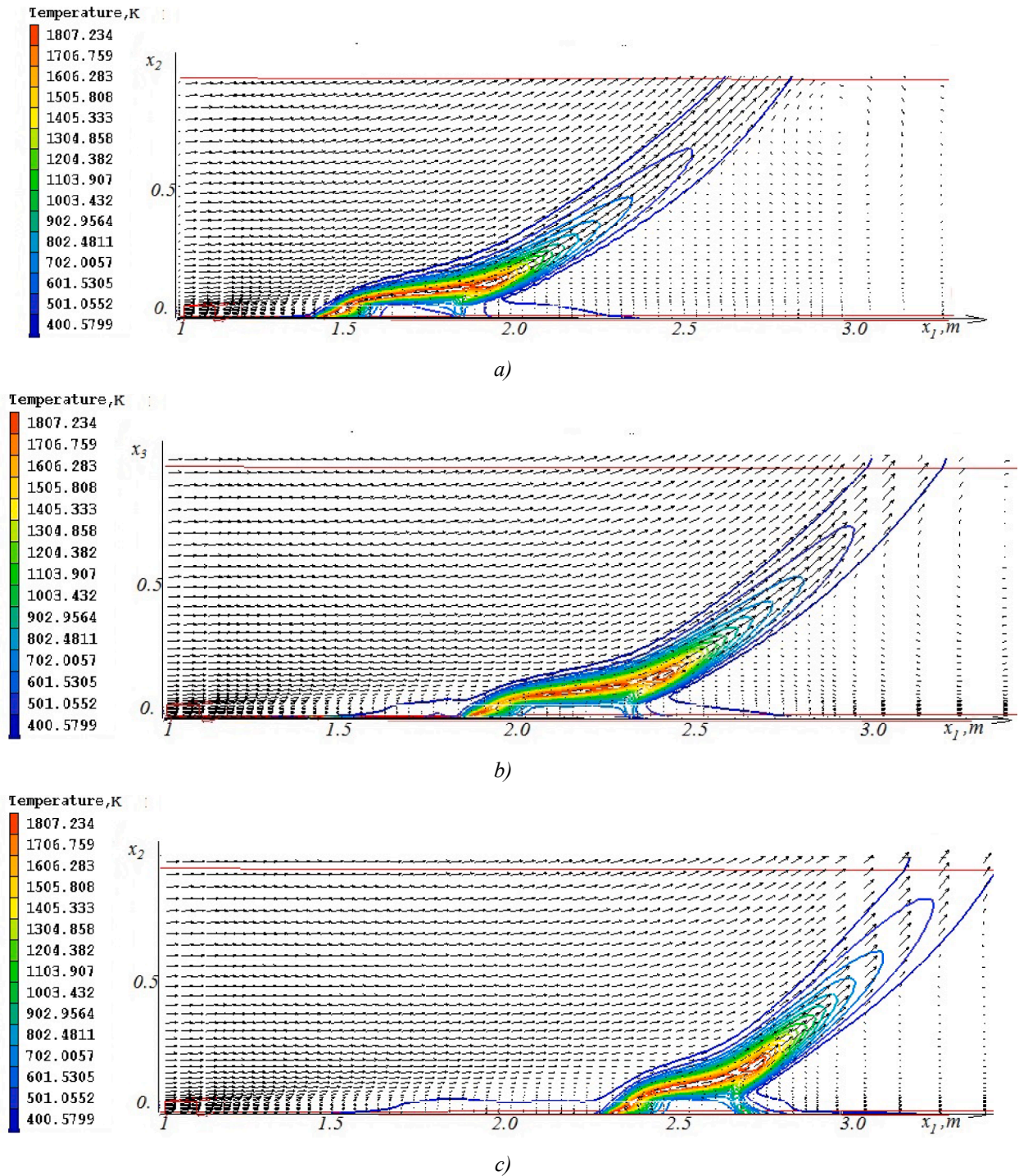


Fig. 6. Gas temperature and velocity vectors at wind speed of 2 m/s.

$$R_2 = k_2 \rho_2 \phi_2 T_s^{-0.5} \exp(-E_2 / RT_s) \quad (7)$$

$$R_3 = k_3 \rho c_1 \sigma_3 \exp(-E_3 / RT_s) \quad (8)$$

Here  $M_1$ ,  $M_2$  and  $M_C$  are the molecular weights of oxygen, carbon monoxide and carbon;  $\alpha_c$  and  $\nu_g$  are the coke number and the fraction of combustible gaseous products of pyrolysis defined by Grishin et al. (1986) and Grishin (1997) ( $\alpha_c = \nu_{char} = 0.06$ ,  $\nu_g = 0.7$ );  $R_1$ ,  $R_2$  and  $R_3$  are the mass rates of chemical reactions (pyrolysis, drying and charcoal combustion) approximated by Arrhenius laws whose parameters, i.e. pre-exponential constants  $k_i$  and activation energies  $E_i$ , are available from Grishin et al. (1986) and Porterie et al. (2000);  $k_1 = 3.63E+4 \text{ s}^{-1}$ ,

$$k_2 = 6 \cdot 10^5 \text{ K}^{1/2} \text{ s}^{-1}, k_3 = 430 \text{ ms}^{-1}, E_1/R = 7250 \text{ K}, E_2/R = 5800 \text{ K}, E_3/R = 9000 \text{ K}.$$

### 2.3. Solid-phase equations

The rates of degradation of condensed phase are computed from the equations (Grishin, 1997):

$$\rho_1 \frac{\partial \phi_1}{\partial t} = -R_1 \quad (9)$$

$$\rho_2 \frac{\partial \phi_2}{\partial t} = -R_2 \quad (10)$$

$$\rho_3 \frac{\partial \phi_3}{\partial t} = \alpha_c R_1 - \frac{M_c}{M_1} R_3 \quad (11)$$

$$\rho_4 \frac{\partial \phi_4}{\partial t} = 0 \quad (12)$$

$$\sum_{i=1}^5 \varphi_i = 1 \quad (13)$$

$$\varphi_s = \sum_{i=1}^4 \varphi_i \quad (14)$$

As suggested by Grishin (1997) and Porterie et al. (2000), the solid particles are considered thermally thin and their temperature is computed from the following conservation equation:

$$\sum_{i=1}^4 \rho_i C_{pi} \phi_i \frac{\partial T_s}{\partial t} = -q_1 R_1 - q_2 R_2 + q_3 R_3 + 4\varepsilon_2 \sigma (T_3^4 - T_s^4) + A_s h_s (T - T_s) \quad (15)$$

Here and above  $\rho_i$ ,  $\varphi_i$  and  $C_{pi}$  are the density, volume fraction and specific heat of a phase component (1 – dry organic substance, 2 – liquid water, 3 – condensed products of pyrolysis, 4 – mineral component of fuel, 5 – gas phase);  $q_i$  are the heat release rates of chemical reactions. In this study, for  $i = 1, 2, 3$  and 4,  $\rho_i = 680, 1000, 200$  and  $200 \text{ kg m}^{-3}$ ;  $C_{pi} = 2.0, 4.18, 0.9$  and  $1.0 \text{ kJ kg}^{-1} \text{ K}^{-1}$ ;  $q_1 = 418 \text{ J kg}^{-1}$  and  $q_3 = 1.2 \cdot 10^7 \text{ J kg}^{-1}$  as proposed by Porterie et al. (2000) and  $q_2 = 3 \cdot 10^6 \text{ J kg}^{-1}$  as suggested by Grishin et al. (1986).

The initial volume fractions of condensed phase are calculated from equations (Grishin et al., 1986):

$$\phi_{1e} = \frac{\rho_0(1 - \nu_{ash})}{\rho_1}, \quad \phi_{2e} = \frac{W\rho_0(1 - \nu_{ash})}{100\rho_2}, \quad \phi_{3e} = 0, \quad \phi_{4e} = \frac{\rho_0\nu_{ash}}{\rho_4} \quad (16)$$

Here,  $\rho_0$  is the bulk density of fuel;  $\nu_{ash}$  is the ashes content ( $\nu_{ash} = 0.04$ );  $W$  is the fuel moisture content (%). In the validation study (section 4),  $\rho_0 = 10 \text{ kg m}^{-3}$ ,  $W = 10\%$ , and equation (16) result in the following initial values of  $\varphi_i$ :  $\varphi_{1e} = 0.014$ ,  $\varphi_{2e} = 9.6 \cdot 10^{-4}$ ,  $\varphi_{4e} = 2 \cdot 10^{-3}$ .

#### 2.4. Radiation model

The radiative transfer equation (RTE) is written with use of a PHOENICS variable,  $T_3$ , defined in [http://www.cham.co.uk/phoenics/d\\_polis/d\\_enc/enc\\_rad3.htm](http://www.cham.co.uk/phoenics/d_polis/d_enc/enc_rad3.htm):

$$\begin{aligned} \frac{\partial}{\partial x_i} \left( \lambda_3 \frac{\partial T_3}{\partial x_i} \right) &= 4\varepsilon_1 \sigma (T_3^4 - T^4) + 4\varepsilon_2 \sigma (T_3^4 - T_s^4); \quad \lambda_3 \\ &= 4\sigma T_3^3 / \left( (0.75(\varepsilon_1 + \varepsilon_2) + 1) / W_{gap} \right) \end{aligned} \quad (17)$$

Here,  $\varepsilon_1$  and  $\varepsilon_2$  are the absorption coefficients of gas and solid phases;  $\varepsilon_1$ , which depends on gas temperature and mass fractions of products of gaseous combustion, was taken equal to a constant value of  $0.1 \text{ m}^{-1}$  for simplicity in this study;  $\varepsilon_2 = \varphi_s \sigma_s / 4 = \varphi_s / d_s$  according to Porterie et al. (1998). Equation (17) is a formulation of the IMMERSOL radiation model as proposed by Spalding (2013). It is similar to RTE in P1-approximation used by Porterie et al. (1998) with the only difference that an additional term,  $1/W_{gap}$ , is included ( $W_{gap}$  is the gap between the solid walls). The presence of the  $1/W_{gap}$  term extends the IMMERSOL model to handle the transparent gases (such as air), i.e. the optically-thin limit ( $\varepsilon_1 = \varepsilon_2 = 0$ ).

### 3. Numerical method

#### 3.1. Solution domain, boundary and initial conditions

The model described in the previous section was validated for a case which was studied experimentally by Mendes-Lopes et al. (2003) and numerically by Porterie et al. (1998, 2000) and Menage et al. (2012). In this case, the fuel bed has the following input parameters (Porterie et al., 1998, 2000): a height of 5 cm, a fuel load value of  $0.5 \text{ kg m}^{-2}$ , a needles density of  $680 \text{ kg m}^{-3}$ , a bulk fuel density of  $10 \text{ kg m}^{-3}$ , an initial moisture content of 10% and a surface-to-volume ratio of needles,  $\sigma_s$ , of about  $5511 \text{ m}^{-1}$ . A  $2.2 \text{ m} \times 1 \text{ m} \times 0.05 \text{ m}$  fuel bed was considered within a  $4.2 \text{ m} \times 1 \text{ m} \times 0.9 \text{ m}$  domain (see Fig. 1).

The governing equations (1)–(17) were solved numerically using PHOENICS CFD solver in its transient mode. At the initial stage, the constant values of all the field variables (pressure, velocity components, phase temperatures and mass fractions) were specified. The wind profile was considered uniform at the flow inlet, i.e. three constant wind speeds of 1, 2 and 3 m/s and a turbulent intensity of 5% were specified at the flow inlet in different runs. The inlet value of turbulence length scale (EL1 variable in PHOENICS) is derived automatically from correlations of RNG  $k-\varepsilon$  turbulence model ([http://www.cham.co.uk/phoenics/d\\_polis/d\\_enc/el1.htm](http://www.cham.co.uk/phoenics/d_polis/d_enc/el1.htm)). The standard wall function approach was used to simulate the gas flow near the domain bottom. Outflow boundary conditions (fixed pressure) were applied at the top and right boundaries of the domain. The default built-in PHOENICS thermal boundary conditions were applied for IMMERSOL model ([http://www.cham.co.uk/phoenics/d\\_polis/d\\_enc/enc\\_rad3.htm#C](http://www.cham.co.uk/phoenics/d_polis/d_enc/enc_rad3.htm#C)).

The ignition source (Ignition Line on Fig. 1) was located at the beginning of fuel bed (at 1 m distance from the origin) and the ignition was simulated by introducing a volumetric heat source of 0.1 m length over the whole fuel bed width and height: the temperature of this region was linearly increased from 700 K to 1000 K during the first 8 s of simulation to generate the heat source required for fuel bed ignition.

#### 3.2. Computational mesh, time discretization and solution convergence

For the sake of simplicity, a 2D formulation was applied by ignoring the gas flow and transport of mass and energy in  $x_2$  direction. A computational grid of  $190 \times 40$  cells was used based on the grid sensitivity study. The grid was non-uniform with a minimum grid size of 5 mm in the fuel bed region. The time step changed from 0.005 s to 0.01 s for different stages of the process. No more than 25 iterations were required to obtain the convergence at each time step. The transient runs were conducted to simulate 90 s of real time. Different grid sizes were tested during the grid sensitivity study and a recommendation by Morvan (2011) was applied: the smallest grid size was less than the extinction length scale  $\delta_R = 4/(\varphi_s \sigma_s) = d_s / \varphi_s$ , which was equal to 43 mm in our study. The time steps were in the range from  $10^{-3}$  to  $10^{-2}$  s (Morvan and Dupuy (2001)).

### 4. Results and discussion

The focus of this study was on the model's capability to predict the fire rate of spread (ROS) measured by Mendes-Lopes et al. (2003) and to reproduce the main flow patterns predicted numerically by Porterie et al. (1998, 2000). The ROS was calculated (in accordance with Porterie et al. (1998, 2000)) as a speed of propagation of the isotherm  $T_s = 600 \text{ K}$  (or 500 K) at the ground level. Fig. 2 shows the transient propagation of pyrolysis front defined with use of isotherm  $T_s = 600 \text{ K}$  for three wind speeds of 1, 2 and 3 m/s. The quasi-steady values of ROS defined as rates of change of front positions with time are 1.2, 2.5 and 4.3 cm/s respectively. These values compare well with the experimental ROS values of Mendes-Lopes et al. (2003) (measured at zero slope of bed): 1.04, 2.08 and 4.92 cm/s respectively.

Figs. 3 and 4 show the distributions of solid phase temperature,  $T_s$ ,

and mass fractions of oxygen ( $C_1$ ) and carbon monoxide ( $C_2$ ) (a gaseous product of pyrolysis) predicted at  $x_3 = 0$  m and  $t = 20$  s for wind speeds of 1 and 2 m/s respectively. The fuel bed heating from propagating fire causes water evaporation, pyrolysis (between 400 K and 500 K) and char combustion (at about 700 K). The carbon monoxide, which is released during pyrolysis, participates in gaseous combustion and its mass fraction drops to zero. The oxygen mass fraction reduces in the pyrolysis zone due to creation of CO in that zone and then it drops to zero within the combustion zone due to oxygen consumption. As the wind velocity increases from 1 to 2 m/s, the width of combustion zone is extended as a result of intensification of heat and mass transfer.

Figs. 5 and 6 show the distributions of gas temperature and velocity predicted at different instants of time (a) -  $t = 20$  s, b) -  $t = 40$  s and c) -  $t = 60$  s) for wind speeds of 1 and 2 m/s respectively. At a wind speed of 1 m/s, a large clockwise eddy is formed ahead of strong buoyant plume and the plume is oscillating with time. As wind speed increases from 1 to 2 m/s, a transition from buoyancy-dominated regime to wind-driven regime is observed and the plume becomes more stable. These flow patterns were also reported by Porterie et al. (2000).

## 5. Conclusions

A multiphase CFD model of wildfire initiation and spread has been developed and incorporated into the multi-purpose CFD software, PHOENICS. The model accounts for all the important physical and physicochemical processes: drying, pyrolysis, char combustion, turbulent combustion of gaseous products of pyrolysis, exchange of mass, momentum and energy between gas and solid phase, turbulent gas flow and convective, conductive and radiative heat transfer. Turbulence is modeled by using the RNG  $k-\epsilon$  model and the radiative heat transfer is approached with the IMMERSOL model (Spalding, 1995, 2013) that is similar to P1-approximation. The Arrhenius-type kinetics is used for heterogeneous reactions (drying, pyrolysis and char combustion) and the eddy dissipation concept is applied for modeling the gaseous combustion. The model was validated using the experimental data of Mendes-Lopes et al. (2003) on surface fire propagation in a bed of *Pinus pinaster* needles studied in a wind tunnel. The predicted rate of spread (ROS) agreed well with experimental values obtained at various wind speeds (from 1 to 3 m/s). The model is being further developed by modifying the radiative heat transfer model and it will be validated using the data on large forest fires including crown fires.

## Declaration of competing interest

The authors declare that they have no known competing financial

interests or personal relationships that could have appeared to influence the work reported in this paper.

## References

- El Houssami, M., Thomas, J.C., Lamorlette, A., Morvan, D., Chaos, M., Hadden, R., Simeoni, A., 2016. Experimental and numerical studies characterizing the burning dynamics of wildland fuels. *Combust. Flame* 168, 113–126.
- El Houssami, M., Lamorlette, A., Morvan, D., Hadden, R.M., Simeoni, A., 2018. Framework for sub-model improvement in wildfire modelling. *Combust. Flame* 190, 12–24.
- Frangieha, N., Morvan, D., Meradjib, S., Accary, G., Bessonov, O., 2018. Numerical simulation of grassland fires behaviour using an implicit physical multiphase model. *Fire Saf. J.* 102, 37–47.
- Grishin, A.M., 1997. In: Albini, F.A. (Ed.), *Mathematical Modeling of Forest Fires and New Methods of Fighting Them*. Tomsk State University Publishing, Tomsk (Russia).
- Grishin, A.M., Zverev, V.G., Shevelev, S.V., 1986. Steady-state propagation of top crown forest fires. *Combust. Explos. Shock Waves* 22, 101–108.
- Lauder, B.E., Spalding, D.B., 1974. The numerical computation of turbulent flows. *Comput. Methods Appl. Mech. Eng.* 3 (2), 269–289.
- Magnussen, B.F., Hjertager, B.H., 1976. On mathematical modeling of turbulent combustion with special emphasis on soot formation and combustion. *Proc. Combust. Inst.* 17, 719–729.
- Mell, W., Jenkins, M.A., Gould, J., Cheney, Ph., 2007. A physics-based approach to modelling grassland fires. *Int. J. Wildland Fire* 16, 1–22.
- Menage, D., Cheteauna, K., Mell, W., 2012. Numerical simulations of fire spread in a *Pinus pinaster* needles fuel bed. In: *Proceedings of 6<sup>th</sup> European Thermal Sciences Conference*. Eurotherm 2012).
- Mendes-Lopes, J.M.C., Ventura, J.M.P., Amaral, J.M.P., 2003. Flame characteristics, temperature-time curves, and rate of spread in fires propagating in a bed of *Pinus pinaster* needles. *Int. J. Wildland Fire* 12, 67–84.
- Morvan, D., 2011. Physical phenomena and length scales governing the behaviour of wildfires: a case for physical modelling. *Fire Technol.* 47, 437–460.
- Morvan, D., Dupuy, J.L., 2001. Modeling of fire spread through a forest fuel bed using a multiphase formulation. *Combust. Flame* 127, 1981–1994.
- Padhi, S., Shotorban, B., Mahalingam, S., 2016. Computational investigation of flame characteristics of a non-propagating shrub fire. *Fire Saf. J.* 81, 64–73.
- Perminov, V., 2013. Mathematical modeling of forest fires propagation taking account of the firebreaks. *Advances in Forestry Letters (AFL)*. 2 (1).
- Porterie, B., Morvan, D., Larini, M., Loraud, J.C., 1998. Wildfire propagation: a two-dimensional multiphase approach. *Combust. Explos. Shock Waves* 34, 26–38.
- Porterie, B., Morvan, D., Larini, M., Loraud, J.C., 2000. Firespread through fuel beds: modeling of wind-aided fires and induced hydrodynamics. *Phys. Fluids* 12, 1762–1782.
- Porterie, B., Consalvi, J.L., Kaiss, A., Loraud, J.C., 2005. Predicting wildland fire behavior and emissions using a fine-scale physical model. *Numer. Heat Tran. Part A: Applications* 47 (6), 571–591.
- Spalding, D.B., 1995. *Modelling Convective, Conductive and Radiative Heat Transfer*. Lecture LE3-1 in *Industrial Computational Fluid Dynamics*. Lecture Series 1995-03. Von Karman Institute for Fluid Dynamics, Belgium. April 3-7.
- Spalding, D.B., 2013. Chapter 1, Trends, tricks, and try-ons in CFD/CHT, Section 3.1. The IMMERSOL radiation model. In: Sparrow, E.M., Cho, Y.I., Abraham, J.P., Gorman, J. M. (Eds.), *Advances in Heat Transfer*, 45. Academic Press, Burlington, pp. 1–78.
- Yakhot, V., Smith, L.M., 1992. The renormalization group, the  $\epsilon$ -expansion and derivation of turbulence models. *J. Sci. Comput.* 7 (1), 35–61.